AIAA JOURNAL
Vol. 38, No. 1, January 2000

Combined Finite Element Analysis and Statistical Energy Analysis in Mechanical Intensity Calculations

Anders M. Wilson* and Lennart B. Josefson†
Chalmers University of Technology, SE-412 96 Gothenburg, Sweden

Local and global energy flow in structures built up by domains with different rigidities is studied. A combined finite element analysis/statistical energy analysis (FEA/SEA) approach is advanced where stiffer domains (with low modal density) are analyzed using FEA and weaker domains (with high modal density) are analyzed using SEA. The approach proposed employs an energy-based iterative optimization procedure where the difference between externally supplied active power and the total power dissipated in the structure is minimized. Sectional forces in points connecting the stiff and weak domains are used as design variables. Dynamic substructuring is introduced to reduce the number of degrees of freedom in the finite element domain during the optimization procedure. The potential to cover a large frequency interval is demonstrated in a numerical example in which the harmonic response of a truck is studied.

Nomenclature

A_s	= source subsystem area
$\boldsymbol{C}$	= damping matrix
c_g	= group wave speed
c_i	= mechanical intensity in direction i
$\boldsymbol{D}(\omega)$	= dynamic stiffness matrix
E	= Young's modulus
$\boldsymbol{E}$ or $\{\boldsymbol{E}\}$	= subsystem modal energy vector
E_i	= average total subsystem i energy
$\boldsymbol{F}$	= force vector
$\boldsymbol{I}$	= unity matrix
i	= $\sqrt{-1}$
$\boldsymbol{K}$	= stiffness matrix
L_x, L_y	= length
$\boldsymbol{M}$	= mass matrix
$N_{\Delta\omega}$	= number of resonant modes in $\Delta\omega$
$n_i(\omega)$	= modal density in subsystem i
$\underline{\boldsymbol{S}}(\omega)$	= complex stiffness matrix
$\boldsymbol{T}$	= transformation matrix
t	= plate thickness
V_{FEM}	= finite element method domain
V_{SEA}	= statistical energy analysis domain
v	= velocity tensor
$\boldsymbol{X}$	= nodal displacement vector
$\dot{\boldsymbol{X}}$	= nodal velocity vector
$\boldsymbol{Z}$	= impedance matrix
$\Delta\omega$	= angular frequency band
ε	= iteration break constant
η	= coupling loss factor matrix
η	= material damping loss factor (DLF)
η_i	= DLF for subsystem i
η_{ij}	= coupling loss factor for energy transfer from subsystem i to j
θ	= angle of incidence
ν	= Poisson's ratio
Π or $\{\Pi\}$	= supplied power vector
Π_i	= power supplied to subsystem i
ρ	= density
σ	= stress tensor
$\tau(\theta)$	= transmission coefficient at an angle of incidence θ
$\boldsymbol{\Phi}$	= fixed interface modal matrix
$\boldsymbol{\Omega}$	= fixed interface natural frequencies matrix
Ω_i	= fixed interface natural frequency
ω	= angular frequency
$\underline{\ }$	= complex entity
$\langle\rangle_\theta$	= average over all angles of incidence θ

Subscripts

m	= reduced matrix/vector representing master degree of freedom (DOF)
mB	= master boundary DOF
mI	= master interface DOF
s	= reduced matrix/vector representing slave DOF

Superscripts

H	= Hermitian transpose (i.e., transpose and complex conjugate)
T	= matrix/vector transpose
$\hat{}$	= starting vector
$\tilde{}$	= approximate vector/matrix
$*$	= complex conjugate

Introduction

FINITE element analysis[1,2] (FEA) is frequently and mostly successfully used to model stress and low-frequency vibration behavior in built-up structures. The method is deterministic. Based on an assumed displacement field of each vibration mode that exists at a certain frequency, each structure can be modeled including coupling between different wave types. Within the level of discretization, the method can provide the vibration amplitude at any point in space and time for any given dynamic input.

By calculating the time average of the complex-valued mechanical intensity in a postprocessing operation also the mechanical energy flow can be visualized,[3] and primary transmission paths for the energy can be identified. For harmonic loading the time average of the complex-valued mechanical intensity is defined as $\underline{c}_i = -1/2\underline{\sigma}^*_{ij}\underline{v}_j$. This energy-based tool may then be used, for example in the early design work, to visualize and control the energy flow in concept models.

Although FEA has proven successful in these areas, it has severe limitations for noise and vibration prediction when the contribution from higher eigenmodes becomes important because of the discretization of the inertia forces where polynomial shape functions are used. For thin-walled steel structures, finite element (FE) calculated results will be poor at about frequencies corresponding to the 10th to 20th eigenmode. The important vibro-acoustic frequency

Presented as Paper 97-1035 at the AIAA/ASME/ASCE/AHS/ASC 38th Structures, Structural Dynamics, and Materials Conference, Kissimmee, FL, 7–10 April 1997; received 27 September 1997; revision received 11 June 1999; accepted for publication 11 June 1999.

*Ph.D. Student, Department of Solid Mechanics: wils@solid.chalmers.se. Member AIAA.
†Professor, Department of Solid Mechanics. Member AIAA.

range, however, often extends beyond the 100th mode of vibration. To further extend the frequency range, in which FEA is acceptably accurate, some form of model reduction may be performed.[4] By using this approach, the number of nodes and elements can be increased, and higher modes may be represented more accurately.

There exist other approaches to extend the frequency range of dynamic FE analyses. One recent example is component mode synthesis,[5] which in Ref. 5 is used to study vibrations in car body structures. However, in principle this approach has the same disadvantage as a FE analysis employing substructuring; it cannot be extended to the high-frequency region in the same manner as a combined FEA and statistical energy analysis (SEA) could.

The SEA[6,7] technique has become increasingly interesting and important as an alternative and a complement to FEA, especially to the aerospace and ship industry, for high-frequency vibration and noise prediction.

The successful application of SEA in its standard form relies on high modal density, high modal overlap, and short wavelengths. These are factors that make FEA inaccurate at high frequencies. Up to now, SEA and FEA have mostly been used separately. But because FEA and SEA have their computational strengths in different frequency ranges, a method of combining these two methods and taking advantage of each method's strengths would be useful. An advantage of a combination of FEA and SEA would be the possibility to analyze a generic structure, which may consist of components or regions having different rigidities. At one frequency, the modal densities of some components could be too high for FEA to be practically applicable, whereas another component is too rigid to permit use of SEA successfully. Coupling between a SEA component and an acoustic cavity is fairly easy, which makes a fluid structure interaction calculation easier. However, using the two methods together is not entirely straightforward because of the differences in the two methods' natures. Some fundamental differences between SEA and FEA are shown in Table 1.

SEA in Brief

SEA is applicable for predicting the average vibro-acoustic behavior of structures in the medium-to-high-frequency region. The SEA approach is based on calculating the power flow between components of a complex mechanical system by analyzing relatively few and low-detail subsystems, which are coupled together. The fundamental element, the subsystem, in the SEA model is a group of similar energy storage blocks. In Fig. 1 a fundamental SEA model built up by two subsystems is shown. These blocks or subsystems usually are modes of the same type (e.g., flexural, torsional, longitudinal) that exist in some section(s) of the components.

The power balance for this system gives

$$\Pi_1 = \omega\eta_1 E_1 + \omega\eta_{12} n_1 (E_1/n_1 - E_2/n_2) \tag{1}$$

$$\Pi_2 = \omega\eta_2 E_2 + \omega\eta_{21} n_2 (E_2/n_2 - E_1/n_1) \tag{2}$$

Table 1 FEA and SEA fundamentals comparison

Criterion	FEA	SEA
Unknown	Displacement	Subsystem energy
Frequency	Discrete, low	Band averge, high
Spatial detail	High, discrete	Low, average
Excitation	Discrete	Average/random/spectrum
Precedure	Complicated, established	Quick, demanding at first
Computational effort	High	Low
Model	Large	Small

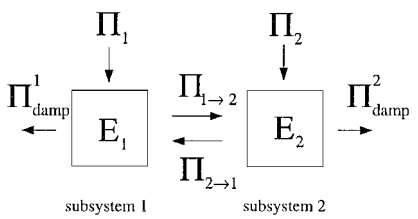

Fig. 1 Fundamental SEA model built up by two subsystems.

The input power may result from acoustic noise or mechanical excitation. The energy in each block may be dissipated by damping, which in each block is described by the damping loss factor (DLF), or transmitted to the neighboring blocks. This energy transmission is proportional to the coupling loss factor (CLF). The modal density, i.e., the average density of resonance frequencies in the frequency band $[n_i(\omega) = N_{\Delta\omega}/\Delta\omega]$, must be high in SEA, which rather can be a problem in FEA. The time-average energy state is obtained by solving the energy balance equations for the system Eqs. (1) and (2). One may note that time-average subsystem energy is the primary unknown in SEA, not nodal displacements amplitudes and phase angles, which is the case in FEA.

Proposed Method

The present work is aimed at combining the two methods of analysis: SEA and FEA. To allow for large FEA models in the analysis, dynamic substructuring[4] is used to reduce the number of degrees of freedom (DOF) in the FE model. In the proposed approach separate SEA and FEA models of different components of the structure are first created. Sectional boundary forces in the model connecting the FEA and SEA components are then iteratively determined so that an objective function, involving the difference between the energy supplied to the structure and the energy dissipated in the structure, is minimized (see also Ref. 8).

Two-Domain Approach

Consider a structure built up by two domains V_{SEA} and V_{FEM} (Fig. 2). The domain V_{SEA} has high modal density and is represented by SEA, and the domain V_{FEM}, the more stiff domain, is modeled by the finite element method (FEM) and reduced using dynamic substructuring.

As indicated in Fig. 2, the two domains are connected along a common boundary. In the FEA domain the connection between the domains is described by connection forces and displacements. Displacements are caused by both external and coupling loads. In the SEA domain the coupling is described by the subsystem energy flow, which in turn is described by power supplied by coupling forces in the interface between the domains. The governing state equations for the two domains are then solved separately at every frequency step, with the common interface forces as iterative variables, until the energy-based objective function is fulfilled.

SEA Domain V_{SEA}

A SEA energy balance for domain V_{SEA} built up by a number of subsystems at the analysis center band frequency ω may be formulated in matrix form according to Eq. (3):

$$\omega[\eta]\{\boldsymbol{E}\} = \{\boldsymbol{\Pi}\} \tag{3}$$

The power input to V_{SEA} is given by

$$\Pi_{in}^{SEA} = \tfrac{1}{2} Re\{\underline{\boldsymbol{F}}_{mI}^{H} \underline{\dot{\boldsymbol{X}}}_{mI}\} \tag{4}$$

where $\underline{\dot{\boldsymbol{X}}}_{mI}$ contains velocity amplitudes of the points of the interface forces and $\underline{\boldsymbol{F}}_{mI}$ contains the corresponding interface force amplitudes. The time average energy state for the system is then obtained by solving the energy balance equation, Eq. (3), at every frequency step, giving the power dissipated in V_{SEA} as a function of $\underline{\boldsymbol{F}}_{mI}$. This force vector is then used in the iterations of the objective function. The size of the matrix and vectors in Eq. (3) is fairly small, due to the fundamental modeling approach in SEA.

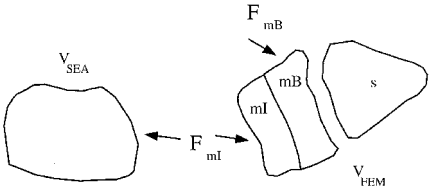

Fig. 2 Domain V_{SEA} analyzed by SEA and domain V_{FEM} with subdomains mI (master interface), mB (master boundary), and s (slave) represented by FEA.

FEA and Dynamic Substructuring of V_{FEM}

The domain V_{FEM}, as shown in Fig. 2, is modeled by FEA. This domain is divided into two subdomains, one with interior slave (index s) DOF $\underline{\boldsymbol{X}}_s$ and one with master boundary DOF (index m) $\underline{\boldsymbol{X}}_m$. The domain m is in turn divided in two subdomains; one subdomain mI in which interface (or coupling) loads are applied and subdomain mB in which external boundary loads are active. The equation of motion for domain V_{FEM} is expressed as

$$\underline{\boldsymbol{D}}(\omega)\begin{Bmatrix}\underline{\boldsymbol{X}}_s\\ \underline{\boldsymbol{X}}_m\end{Bmatrix}=\begin{Bmatrix}\underline{\boldsymbol{F}}_s\\ \underline{\boldsymbol{F}}_m\end{Bmatrix} \tag{5}$$

or if divided into subdomains as

$$\underline{\boldsymbol{D}}(\omega)\begin{Bmatrix}\underline{\boldsymbol{X}}_s\\ \underline{\boldsymbol{X}}_{\text{mB}}\\ \underline{\boldsymbol{X}}_{\text{mI}}\end{Bmatrix}=\begin{Bmatrix}\underline{\boldsymbol{F}}_s\\ \underline{\boldsymbol{F}}_{\text{mB}}\\ \underline{\boldsymbol{F}}_{\text{mI}}\end{Bmatrix} \tag{6}$$

The reason for dividing the domain V_{FEM} into two areas is to eliminate the (slave) DOF that are of no primary interest in the analysis to reduce the number of active DOF in the optimization procedure described next.

There are a great variety of dynamic substructuring reduction methods available. Generally, for an undamped system under harmonic load with angular frequency ω, the system of equations for the domain containing $\underline{\boldsymbol{X}}_m$ can be partitioned into parts containing the slave DOF and the master DOF. When assuming that no loads are applied to the eliminated slave degrees of freedom, $\boldsymbol{F}_s = 0$, the partitioned system of equations may be written as

$$\begin{bmatrix}\boldsymbol{D}_{\text{ss}} & \boldsymbol{D}_{\text{sm}}\\ \boldsymbol{D}_{\text{ms}} & \boldsymbol{D}_{\text{mm}}\end{bmatrix}\begin{Bmatrix}\boldsymbol{X}_s\\ \boldsymbol{X}_m\end{Bmatrix}=\begin{Bmatrix}0\\ \boldsymbol{F}_m\end{Bmatrix} \tag{7}$$

with

$$\boldsymbol{D}_{\text{ss}} = \boldsymbol{K}_{\text{ss}} - \omega^2\boldsymbol{M}_{\text{ss}}, \qquad \boldsymbol{D}_{\text{sm}} = \boldsymbol{K}_{\text{sm}} - \omega^2\boldsymbol{M}_{\text{sm}}$$
$$\boldsymbol{D}_{\text{mm}} = \boldsymbol{K}_{\text{mm}} - \omega^2\boldsymbol{M}_{\text{mm}}, \qquad \boldsymbol{D}_{\text{ms}} = \boldsymbol{D}_{\text{sm}}^T \tag{8}$$

An exact dynamic representation of an undamped substructure is given by the reduced system of equations in Eq. (9):

$$(\boldsymbol{K}_m - \omega^2\boldsymbol{M}_m)\boldsymbol{X}_m = \boldsymbol{D}_m\boldsymbol{X}_m = \boldsymbol{F}_m \tag{9}$$

The exact reduced stiffness and mass matrixes in Eq. (9) are given by a matrix transformation, according to Eqs. (10–12):

$$\boldsymbol{K}_m = \boldsymbol{T}^T\boldsymbol{K}\boldsymbol{T} \tag{10}$$

$$\boldsymbol{M}_m = \boldsymbol{T}^T\boldsymbol{M}\boldsymbol{T} \tag{11}$$

$$\boldsymbol{T} = \begin{bmatrix}-\boldsymbol{D}_{\text{ss}}^{-1}\boldsymbol{D}_{\text{sm}}\\ \boldsymbol{I}\end{bmatrix} \tag{12}$$

where the transformation matrix $\boldsymbol{T}$ is used to recover the complete solution as

$$\begin{Bmatrix}\boldsymbol{X}_s\\ \boldsymbol{X}_m\end{Bmatrix}=\boldsymbol{T}\boldsymbol{X}_m \tag{13}$$

However, the inverse of the matrix $\boldsymbol{D}_{\text{ss}}$ in Eq. (12), which has to be computed at every analysis frequency, is computationally quite expensive to calculate. Because the system is undamped, one has exact by expansion[4,9]

$$\boldsymbol{D}_{\text{ss}}^{-1}(\omega) = \boldsymbol{K}_{\text{ss}}^{-1} + \omega^2\boldsymbol{K}_{\text{ss}}^{-1}\boldsymbol{M}_{\text{ss}}\boldsymbol{K}_{\text{ss}}^{-1} + \omega^4\boldsymbol{\Phi}\,\text{diag}_{i=1:n}\left[\Omega_i^{-4}(\Omega_i^2-\omega^2)^{-1}\boldsymbol{I}\right]\boldsymbol{\Phi}^T \tag{14}$$

where $\boldsymbol{\Omega}^2 = \text{diag}[\Omega_1^2, \Omega_2^2, \ldots, \Omega_n^2]$ contains the n undamped fixed interface natural frequencies and $\boldsymbol{\Phi}$ is the corresponding undamped fixed interface modal matrix. This means that $\boldsymbol{\Omega}$ and $\boldsymbol{\Phi}$ are calculated for the case when the master degrees of freedom are constrained and normalized so that

$$\boldsymbol{\Phi}^T\boldsymbol{M}_{\text{ss}}\boldsymbol{\Phi} = \boldsymbol{I} \tag{15}$$

$$\boldsymbol{\Phi}^T\boldsymbol{K}_{\text{ss}}\boldsymbol{\Phi} = \boldsymbol{\Omega}^2 \tag{16}$$

The undamped fixed interface modes may be calculated by an Arnoldi algorithm with spectral transformation.[10]

If not all n fixed interface modes are included in $\boldsymbol{\Phi}$, the expression for $\boldsymbol{D}_{\text{ss}}^{-1}$, Eq. (14) may be truncated at eigenpair p as

$$\tilde{\boldsymbol{D}}_{\text{ss}}^{-1}(\omega) = \boldsymbol{K}_{\text{ss}}^{-1} + \omega^2\boldsymbol{K}_{\text{ss}}^{-1}\boldsymbol{M}_{\text{ss}}\boldsymbol{K}_{\text{ss}}^{-1} + \omega^4\boldsymbol{\Phi}\,\text{diag}_{i=1:p}\left[\Omega_i^{-4}(\Omega_i^2-\omega^2)^{-1}\boldsymbol{I}\right]\boldsymbol{\Phi}^T \tag{17}$$

where $p < n$. The truncation gives an approximate transformation matrix $\tilde{\boldsymbol{T}}$. The solution is then obtained as in Eqs. (18–20):

$$\tilde{\boldsymbol{K}}_m = \tilde{\boldsymbol{T}}^T\boldsymbol{K}\tilde{\boldsymbol{T}} \tag{18}$$

$$\tilde{\boldsymbol{M}}_m = \tilde{\boldsymbol{T}}^T\boldsymbol{M}\tilde{\boldsymbol{T}} \tag{19}$$

$$(\tilde{\boldsymbol{K}}_m - \omega^2\tilde{\boldsymbol{M}}_m)\tilde{\boldsymbol{X}}_m = \tilde{\boldsymbol{D}}_m\tilde{\boldsymbol{X}}_m = \boldsymbol{F}_m \tag{20}$$

Accurate results may be achieved despite the approximation introduced by the truncation in Eq. (17). Reference 11 has indicated that the number of modes to include in Eq. (17) is dependent on the analysis frequency. Fixed interface modes with corresponding natural frequencies approximately up to the analysis frequency should be included to keep the truncation error small.

Coupling of the FEA and SEA Domains

To obtain a solution, the complex amplitudes of the master interface forces $\underline{\boldsymbol{F}}_{\text{mI}}$ are chosen as design variables at the coupling points connecting the V_{SEA} and V_{FEM} domains. For the V_{FEM} domain these forces will act as external forces (together with the boundary forces $\underline{\boldsymbol{F}}_{\text{mB}}$ that supply the input power to the stiff component). At each frequency ω the complex harmonic response at the interface DOF $\underline{\boldsymbol{X}}_{\text{mI}}$ is calculated using the reduced form of Eqs. (6) and (20), assuming $\boldsymbol{F}_s = 0$. For the same frequency a SEA calculation is performed for the weak component subject to an energy input at the connecting points, determined by the current values of $\underline{\boldsymbol{F}}_{\text{mI}}$ and the impedance corresponding to $\underline{\boldsymbol{X}}_{\text{mI}}$. In an iterative procedure the magnitudes and phases (e.g., $\underline{\boldsymbol{F}}_{\text{mI}}$ is complex) of the forces $\underline{\boldsymbol{F}}_{\text{mI}}$ are varied until the following objective function is minimized:

$$\min_{\underline{\boldsymbol{F}}_{\text{mI}}}\left|\frac{\Pi_{\text{in}} - \Pi_{\text{damp}}}{\Pi_{\text{in}}}\right| \le \varepsilon \tag{21}$$

where $\varepsilon \ll 1$.

The power expressions in Eq. (21) are

$$\Pi_{\text{in}} = \tfrac{1}{2}Re\left\{\underline{\boldsymbol{F}}_{\text{mB}}^H\dot{\underline{\boldsymbol{X}}}\right\} \tag{22}$$

which is the energy input to the structure V_{FEA} by external boundary forces $\underline{\boldsymbol{F}}_{\text{mB}}$ and Π_{damp} is the sum of the energy dissipated in the stiff component:

$$\Pi_{\text{damp}}^{V_{\text{FEM}}} = \tfrac{1}{2}Re\left\{\dot{\underline{\boldsymbol{X}}}^H\boldsymbol{C}_m\dot{\underline{\boldsymbol{X}}}\right\} \tag{23}$$

and in the weak component:

$$\Pi_{\text{damp}}^{V_{\text{SEA}}} = \sum_i E_i\omega\eta_i \tag{24}$$

The displacements at the interface between V_{FEM} and V_{SEA}, $\underline{\boldsymbol{X}}_{\text{mI}}$, are calculated from the FE analysis of V_{FEM} and used, together with the design forces $\underline{\boldsymbol{F}}_{\text{mI}}$, to obtain the subsystem energies E_i in V_{SEA}.

The calculation of the starting vector of the unknown force amplitudes $\hat{\underline{\boldsymbol{F}}}_{\text{mI}}$ in the optimization process is based in the impedance for infinite structures[12] connected to the FE model. These approximate subsystems are chosen as the same type of subsystems as those of the actual connected V_{SEA} domain.

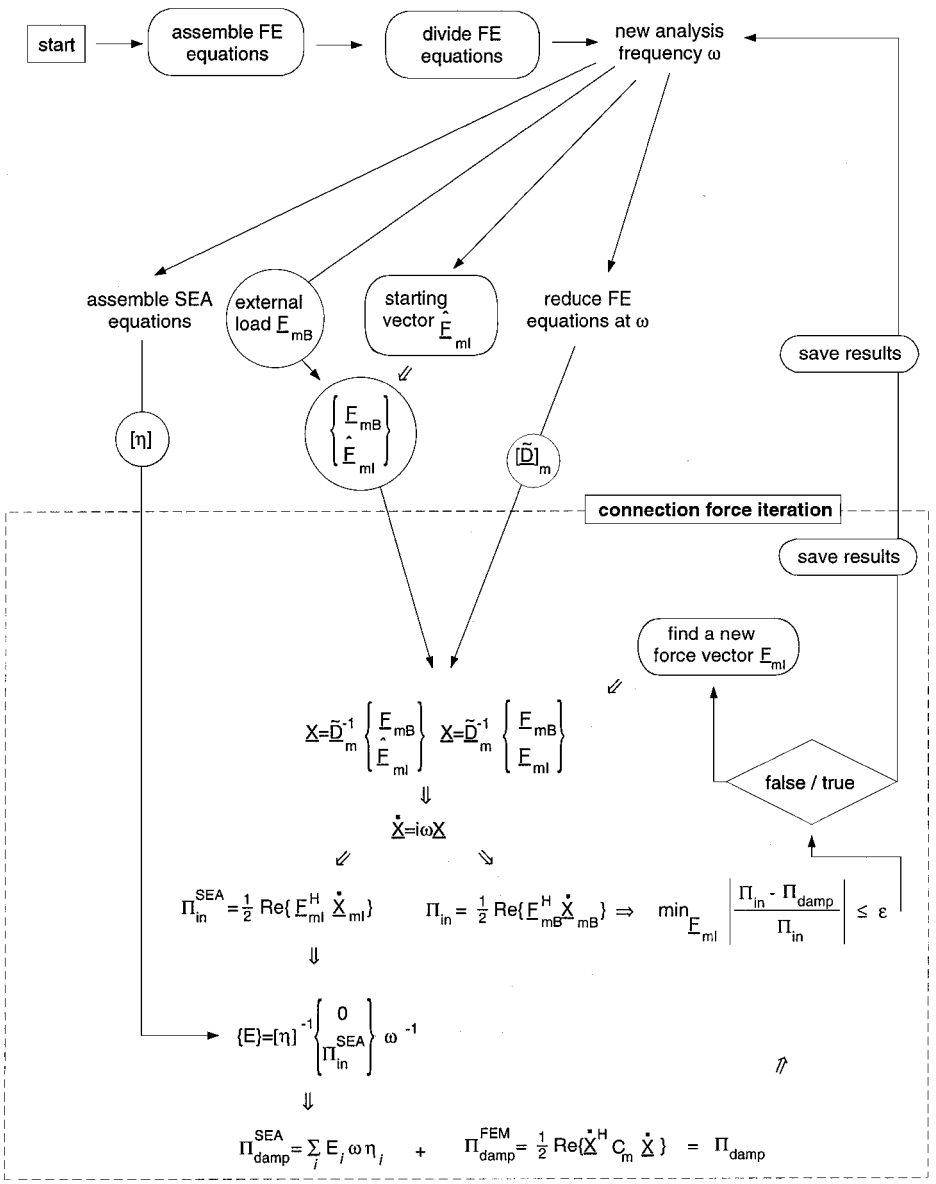

Fig. 3 Calculation scheme used for the minimization procedure.

The complete reduced starting system of equations may be written in terms of some unknown coupling displacements $\hat{\underline{X}}_{mI}$ and forces $\hat{\underline{F}}_{mI}$ as

$$\underline{D}(\omega)_m \begin{Bmatrix} \underline{X}_{mB} \\ \hat{\underline{X}}_{mI} \end{Bmatrix} = \begin{Bmatrix} \underline{F}_{mB} \\ \hat{\underline{F}}_{mI} \end{Bmatrix} \tag{25}$$

Using the expression for the impedance $\boldsymbol{Z}$ for the connected approximate SEA subsystems (to approximate the connection between the FEA and the SEA domains), Eq. (25) may be rewritten as

$$\underline{D}(\omega)_m \begin{Bmatrix} \underline{X}_{mB} \\ \hat{\underline{X}}_{mI} \end{Bmatrix} = Zi\omega \begin{Bmatrix} 0 \\ \hat{\underline{X}}_{mI} \end{Bmatrix} + \begin{Bmatrix} \underline{F}_{mB} \\ 0 \end{Bmatrix} \tag{26}$$

which can be solved for the unknown coupling displacements $\hat{\underline{X}}_{mI}$. This in turn gives the starting forces $\hat{\underline{F}}_{mI}$ as $\hat{\underline{F}}_{mI} = i\omega Z \hat{\underline{X}}_{mI}$.

The minimization is performed in MATLAB®[13] using the fmins function, thus employing an iterative Broyden–Fletcher–Goldfarb–Shanno (BFGS) quasi-Newton minimization with a mixed quadratic and cubic line search procedure. This is run until the objective function in Eq. (21) is satisfied. Because dynamic substructuring is employed, the size of the problem used in the iterations, to fulfill the energy balance for the structure, is fairly small.

The calculation scheme used for the minimization procedure, where the objective function in Eq. (21) is fulfilled, is described in Fig. 3.

Numerical Example: Truck Structure

To investigate the method proposed, a harmonic vibration analysis of a structure built up by one stiff and one weak domain connected at a number of discrete points is performed.

The structure analyzed is to resemble a conceptual model of a truck structure as shown in Fig. 4. In the model the frame and engine constitutes the stiff domain V_{FEM} having 21 eigenmodes up to 100 Hz. The weak domain V_{SEA} is here the cabin, which has more than 20 eigenmodes below 10 Hz. The truck is excited at the engine by a vertical point force.

FE Model of Frame

The frame, as shown in Figs. 4 and 5, is modeled by 138 two-node Timoshenko beam elements. This part of the structure is taken as undamped. The wheel suspension is modeled as 8×3 two-node spring elements with translational stiffness in three directions and hysteretic damping in the vertical direction with loss factor $\eta = 0.05$. The frame-to-cabin connection is modeled by two-node connection springs at four locations. These springs have translational and rotational stiffness in three directions, respectively, and translational

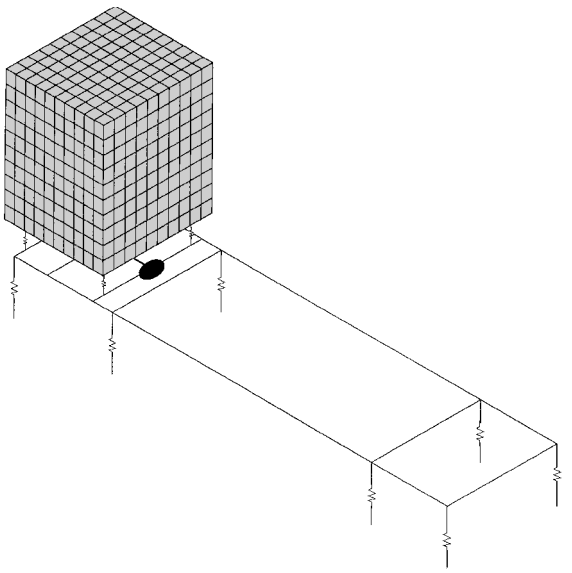

Fig. 4 FEA model of truck structure consisting of engine, frame, suspension, and cabin.

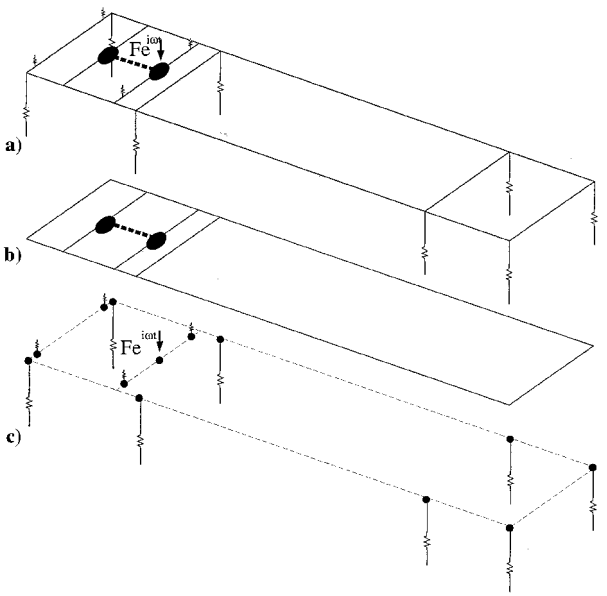

Fig. 5 Frame structure: a) complete FEA model of engine and frame structure used in numerical example, b) unreduced (undamped) frame structure, and c) reduced FEA model (dashed) with retained nodes (dots) (damped springs added).

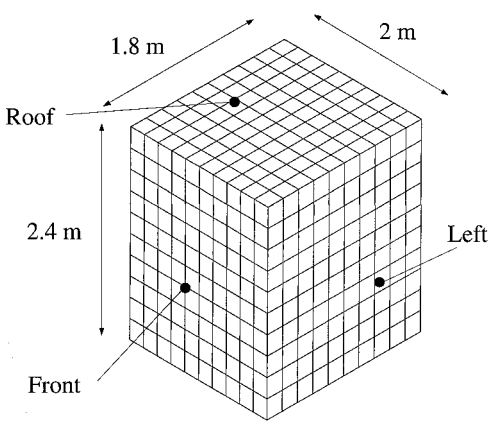

Fig. 6 Reference cabin FE model A containing 600 four-node shell elements.

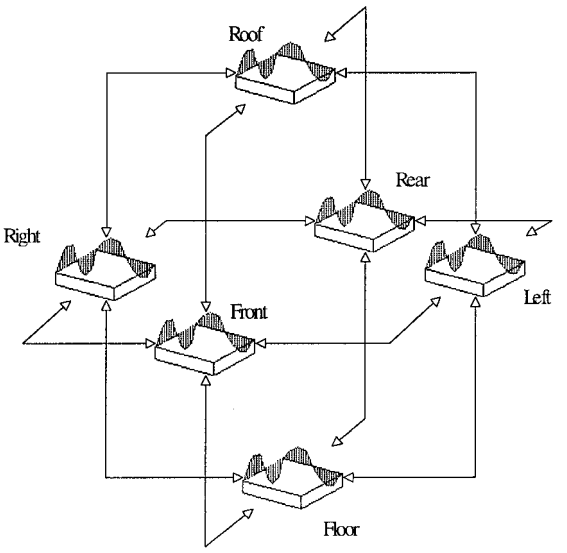

Fig. 7 SEA network of cabin built up by six subsystems representing flexural modes in thin plates.

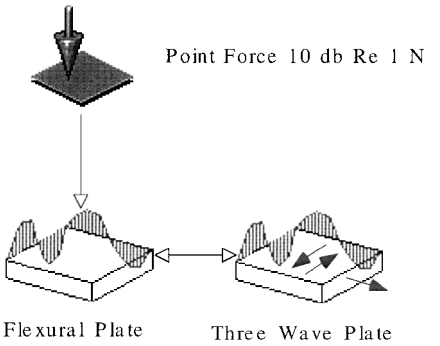

Fig. 8 Example network used to validate assumption used when modeling with SEA.

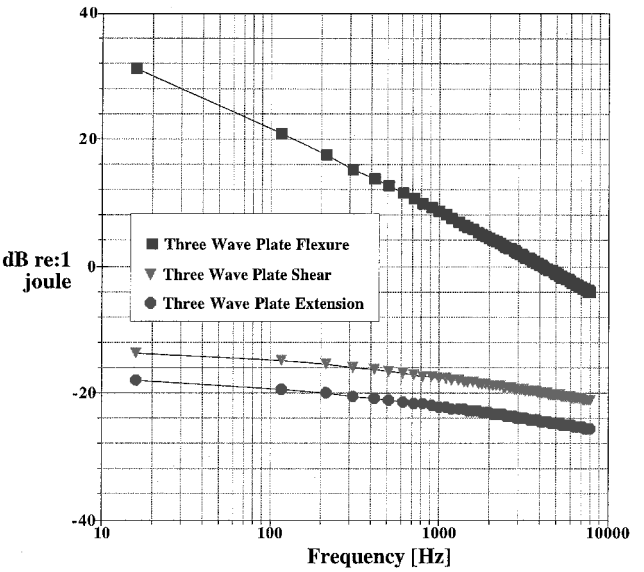

Fig. 9 Power supplied to a three-wave-type plate through a perpendicular flexural plate by a point force. Subsystem network shown in Fig. 8.

hysteretic damping, with $\eta = 0.08$ in the vertical direction. Concentrated 100-kg masses are added at the four connection points. The engine is modeled as two rigidly connected 500-kg concentrated masses.

As just discussed, to perform many solution steps efficiently the frame structure shown in Fig. 5a is reduced using the approximate dynamic substructuring approach, Eqs. (17–20). The undamped frame (Fig. 5b) is reduced, retaining the node of load application (at

the engine), the wheel suspension spring element connection nodes, and the cabin-to-frame connection nodes (where damping is introduced). Totally 13 nodes of 146 are retained. The reduced FE model is shown in Fig. 5c. It is in the frame-to-cabin connection nodes that the iteration forces $\underline{\boldsymbol{F}}_{\mathrm{mI}}$ are introduced.

SEA Cabin Model

The cabin is here modeled by SEA subsystems because it has a large number of resonant modes at low frequencies. The cabin is built up from the geometry in Fig. 6 and represented by a number of subsystems; six flexural plates according to Fig. 7. The cabin is modeled in the commercial SEA software AutoSea,[6] by which the SEA parameters (coupling loss factors, modal densities, etc.) are calculated. Material parameters used in the cabin and in the frame should resemble steel with Young's modulus $=207$ MPa, density $=7820$ kg/m^3, and Poisson's ratio $=0.29$. The plate thickness is 2 mm. The cabin is taken as hysteretically damped with a constant damping loss factor $\eta=0.01$. To fully model the plates used in the model, all three wave types should be included, i.e., flexural, extensional, and shear waves. However, when calculating the number of modes in the frequency bands, as defined in Eqs. (27–29), the number of resonant excited modes is substantially lower for the shear and extensional waves compared to the flexural waves. This means that the SEA assumptions are not valid at low frequencies for these two types of subsystems:

$$n_{\mathrm{flex}} = \frac{L_x L_y}{4\pi}\sqrt{\frac{\rho t}{[Et^3/12(1-\nu^2)]}} \tag{27}$$

$$n_{\mathrm{ext}}(\omega) = \frac{L_x L_y}{4\pi}\sqrt{\frac{\omega}{[E/\rho(1-\nu^2)]}} \tag{28}$$

$$n_{\mathrm{shear}}(\omega) = (L_x L_y/4\pi)[\omega/(G/\rho)] \tag{29}$$

To investigate the validity of only including the flexural modes, one may calculate the power supplied to a three-wave-type plate subsystem through a perpendicular flexural plate by a point force (which is similar to the subsystem network in the numerical example), as shown in Fig. 8. Calculating the vibrational energy for the different wave types in the three-wave-type plate (Fig. 9) shows that the main part of vibrational energy is stored in flexural modes, which indicates that the assumption to include only these modes in the subsystem network is reasonable.

For the structure used in this analysis, one of the criteria for SEA to be valid (i.e., the number of modes in band being $\gg 1$) is well met for the flexural wave type. For the plates in the SEA model, the number of modes in band are for the front/rear 784, left/right 700, and floor/roof 580, for a frequency band $\Delta\omega = 100$ Hz.

The subsystems are coupled along the connecting lines, where the average CLF for plate-to-plate is given by Eqs. (30) and (31):

$$\eta_{12} = (c_g L_x/\pi\omega A_s)\langle\tau(\theta)\cos(\theta)\rangle_\theta \tag{30}$$

$$\langle\tau(\theta)\cos\theta\rangle_\theta = \frac{1}{\pi}\int_{-\pi/2}^{\pi/2}\tau(\theta)\cos\theta\,\mathrm{d}\theta \tag{31}$$

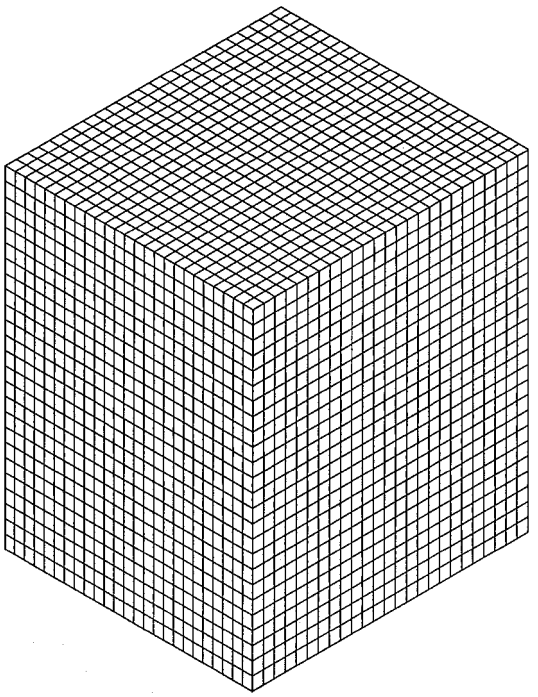

Fig. 10 Reference model B: FE model containing 3936 four-node shell elements.

Reference Cabin FE Model

Reference solution models, where both the frame and the cabin are modeled using FEA, are obtained using the commercial FE code

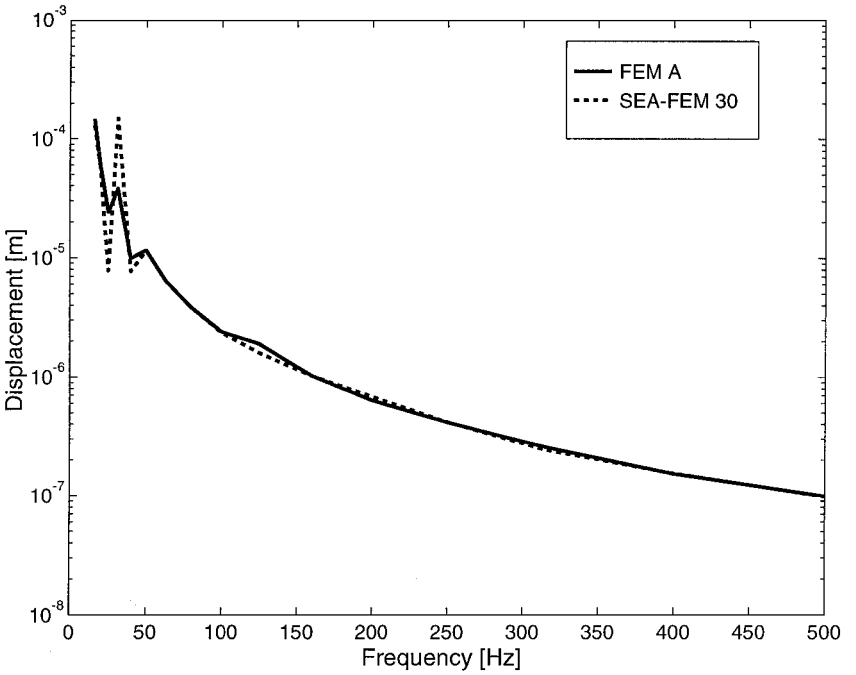

Fig. 11 Calculated frequency variation of the real part of the vertical displacement at the load application point on the frame. Thirty fixed interface modes are included in substructuring of frame used in combined FEA/SEA model. Compared with reference model A.

SOLVIA.[14] The model of the frame, engine, and suspension is the same as already described, and the cabin is modeled in two reference models. Reference model A has 600 iso-parametric four-node shell elements of Mindlin type (see mesh in Fig. 6) and reference model B has 3936 elements of the same kind (see Fig. 10). The element size used is 0.20 m in reference model A and 0.08 m in reference model B, which gives a maximum reliable frequency[15] of 61 and 380 Hz with four elements/wavelength, respectively.

Calculated Results

Figure 11 shows the calculated frequency variation of the real part of the amplitude of the vertical displacement at the point of load application. Results using the FEA/SEA approach, using dynamic substructuring with 30 undamped fixed interface modes (with the highest mode corresponding to 150 Hz) included in the reduction, are compared with results from the full reference A FE model. One finds that the FEA/SEA approach seems to miss two resonances: FEA mode 5 at 25 Hz and mode 7 at 30 Hz. These modes involve in-plane motion in the floor. Otherwise the agreement is good.

Figure 12 shows the calculated frequency variation of the real part of the power supplied to the truck structure, that is, the active power input using the present FEA/SEA approach compared to using the reference FEA models A and B with the cabin modeled using some 600 and 3936 shell finite elements, respectively. For the FEA/SEA approach results are presented for three different levels of dynamic substructuring, including 10, 30, and 60 fixed interface

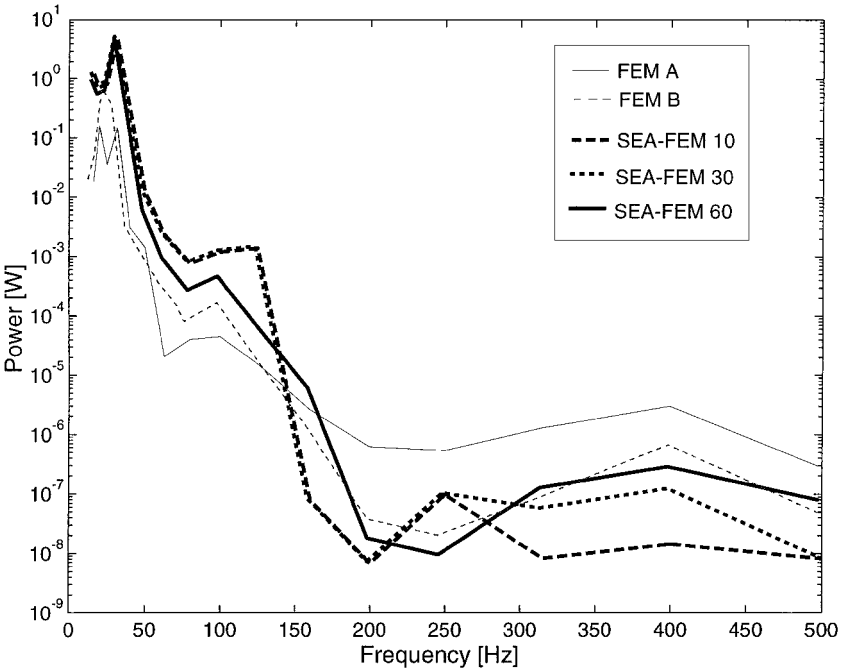

Fig. 12 Calculated frequency variation of the real part of the supplied power to the truck structure. Different number of fixed interface modes used in substructuring of FE part. Compared with reference models A and B.

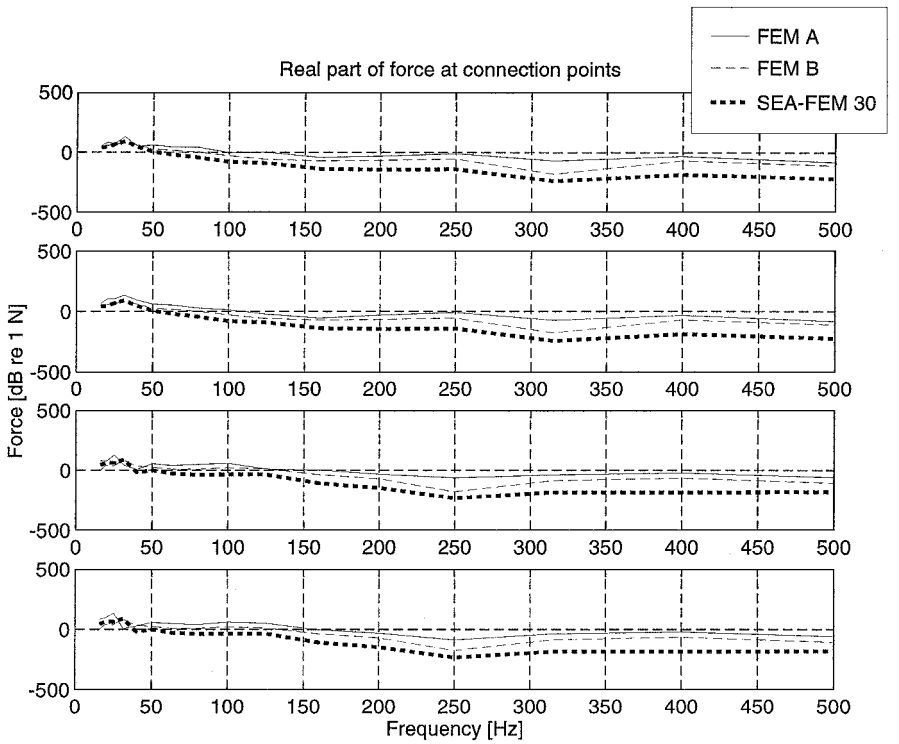

Fig. 13 Calculated frequency variation of the magnitude of the real part of the forces connecting the truck structure and the cabin. Thirty fixed interface modes are included in substructuring of frame. Compared with reference models A and B.

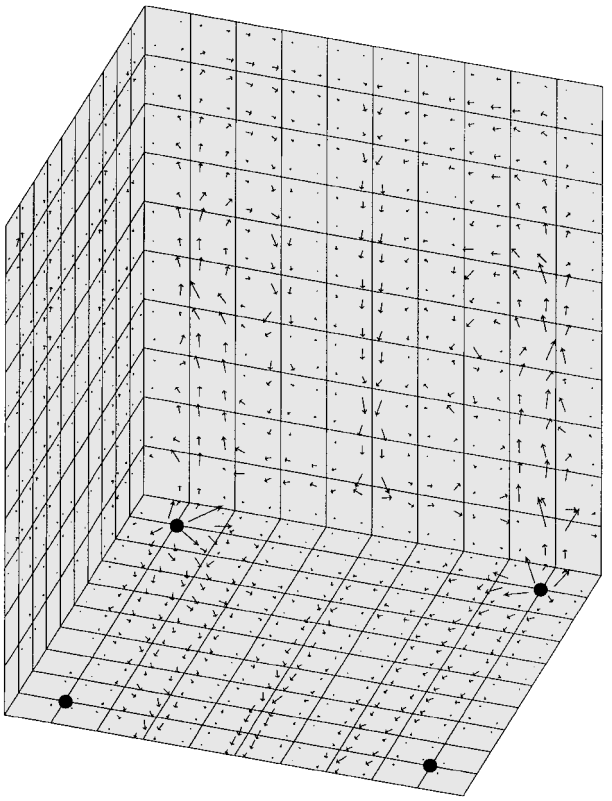

Fig. 14 Calculated real part of the mechanical intensity vector field in the cabin part of reference model A at one low-resonance frequency (100 Hz): front view, looking up at the connection points (marked).

modes corresponding to eigenfrequencies at 51, 150, and 300 Hz, respectively, in the reduction of the frame structure.

One finds good agreement between the FEA/SEA approach and the reference A model up to frequencies of approximately 60 Hz, where the cabin part of the reference FE model becomes inaccurate. When comparing to reference model B, which is valid up until approximately 380 Hz, one finds that including more interface modes in the reduction does seem to extend the validity of the calculated frequency response.

Figure 13 shows the calculated frequency variation of the magnitudes of the four cabin-to-frame connection forces. The results from the FEA/SEA approach (using dynamic substructuring with 30 interface modes included in the reduction), where the connection forces are used as design variables, are compared with the results for reference models A and B. Reference models A and B should give good agreement, at least up to approximately 60 and 380 Hz, respectively.

Note, however, that there exist no exact reference solutions to the present problem for the frequency range plotted. Such a solution would require a much denser FE mesh of the cabin part, or experimental verification.

Figure 14 shows the calculated real part of the mechanical intensity vector field in the cabin plates at one low resonance frequency. These results are obtained from the reference FE model A of the truck using the commercial FE code SOLVIA.[14] Transmission of energy from the frame-to-cabin connections to the cabin is clearly displayed.

Conclusions

By combining a FEA and a SEA, it seems possible to use the advantages of both approaches and obtain a harmonic response over a large frequency interval. The present approach is particularly useful when the structure analyzed consists of domains having considerably different rigidities. The state description of the structure is more detailed in FEA than in SEA. Because SEA is based on energy transfer, phase angles for displacements and forces are not included in the SEA model. Because this information needs to be included in a FE analysis, the present approach to couple a FEA and a SEA model involves minimization of the difference between the total power input to the structure and the total power dissipated within the structure. The procedure is iterative at each frequency. It is therefore desirable to employ dynamic substructuring in the FE model in order to reduce the size of the model involved in the minimization procedure. The results show that dynamic substructuring may be used to reduce the size of the FEA domain system of equations when care is taken as to which modes are included in the reduced model. As the mesh of the FE-modeled domain is made more dense, the results at high frequencies from the combined model get more similar to those of a pure FE reference model. However, it is believed that the present approach in some aspects need to be further developed; the optimal level of substructuring in the FE model and the use of robust starting vectors for the design variables in the iterative minimization procedure need to be further investigated

Acknowledgments

The work presented was funded by the Swedish Research Council for Engineering Sciences through Contract 94-300 and by Volvo Corporation, Göteborg, Sweden, through the Volvo–Chalmers Vehicle Research Program. Special thanks to Mikael Enelund at the Department of Solid Mechanics, Chalmers University of Technology.

References

[1]Bathe, K.-J., *Finite Element Procedures*, Prentice–Hall, Upper Saddle River, NJ, 1996.

[2]Cook, R. D., Malkus, D. S., and Plesha, M. E., *Concepts and Applications of Finite Element Analysis*, 3rd ed., Wiley, New York, 1989.

[3]Alfredsson, K. S., Josefson, B. L., and Wilson, M. A., "Use of the Energy Flow Concept in Vibration Design," *AIAA Journal*, Vol. 34, No. 6, 1996, pp. 1250–1255.

[4]Wilson, M. A., and Josefson, B. L., "Mechanical Intensity Fields in Reduced Structures," *Proceedings of the AIAA/ASME/ASCE/AHS/ASC 37th Structures, Structural Dynamics, and Materials Conference*, Pt. 2, AIAA, Reston, VA, 1996, pp. 1585–1593.

[5]Ichikawa, T., and Hagiwara, I., "Frequency Response Analysis of Large-Scale Damped Structures Using Component Mode Synthesis," *Japan Society of Mechanical Engineering International, Series C*, Vol. 39, No. 3, 1996, pp. 450–455.

[6]*AutoSea User Guide Rev. 1.4*, Vibro-Acoustics Sciences Ltd., San Diego, CA, 1996.

[7]Lyon, R. H., and DeJong, R. G., *Theory and Application of Statistical Energy Analysis*, 2nd ed., Butterworth–Heinemann, Newton, MA, 1995.

[8]Lu, L., "Dynamic Substucturing by FEA/SEA," *Proceedings of Vehicle Noise*, Vol. NCA-9, American Society of Mechanical Engineers, New York, 1990, pp. 9–12.

[9]Leung, A. Y. T., *Dynamic Stiffness and Substructures*, Springer–Verlag, London, 1993, p. 73.

[10]Ericsson, T., and Ruhe, A., "The Spectral Transformation for the Numerical Solution of Large Sparse Generalized Symmetric Eigenvalue Problems," *Mathematics of Computation*, Vol. 35, No. 152, 1980, pp. 1251–1268.

[11]Wilson, M. A., "Extended Frequency Range for Finite Element Based Vibration Analysis," Lic. Eng. Thesis, Rept. 1997:3, Div. of Solid Mechanics, Chalmers Univ. of Technology, Göteborg, Sweden, May 1997.

[12]Cremer, L., Heckl, M., and Ungar, E. E., *Structure-Bourne Sound*, 2nd ed., Springer–Verlag, Berlin, 1988, p. 290.

[13]*MATLAB Reference Guide*, MathWorks, Inc., Natick, MA, 1993.

[14]*SOLVIA-PRE 95.0 Users Manual for Stress Analysis*, Solvia Engineering AB, Västerås, Sweden, 1995.

[15]Blevins, R. D., *Formulas for Natural Frequency and Mode Shape*, Van Nostrand Reinhold Co., New York, 1979, p. 258.

R. K. Kapania
Associate Editor